Role of Maraviroc and/or Rapamycin in Aging Liver Processes

Laura Perez Martinez (lperez@riojasalud.es)
CIBIR: Centro de Investigacion Biomedica de La Rioja https://orcid.org/0000-0002-1384-024X
Lourdes Romero
CIBIR: Centro de Investigacion Biomedica de La Rioja
Eva M Verdugo-Sivianes
Instituto de Biomedicina de Sevilla
Sandra Muñoz-Galvan
Instituto de Biomedicina de Sevilla
Susana Rubio-Mediavilla
Hospital San Pedro
Ana Amiama
CIBIR: Centro de Investigacion Biomedica de La Rioja
Amancio Carnero
Instituto de Biomedicina de Sevilla
Jose Ramon Blanco
CIBIR: Centro de Investigacion Biomedica de La Rioja

Research

Keywords: Liver, CCR5 antagonist, aging, maraviroc, rapamycin

Posted Date: June 3rd, 2022

DOI: https://doi.org/10.21203/rs.3.rs-1669382/v1

Abstract

Background: Cellular senescence and low-grade inflammation favor the acceleration of aging. The liver is an essential metabolic organ because changes related to its function are related to age-related diseases. The objective of this study was to evaluate the effects of maraviroc (MVC) and/or rapamycin (RAPA) on liver tissue in an experimental model of aging in mice.

Materials and methods: Eighty male homozygous IL10KO mice were randomly assigned to one of 4 groups (n= 20): i) IL10KO group (IL10KO); ii) IL10KO mice that received MVC in drinking water (MVC group), iii) IL10KO mice that received RAPA in drinking water (RAPA group), and iv) MVC-RAPA group that received MVC and RAPA in drinking water. Liver samples were analyzed. Gene expression quantification, western blotting and histopathological analyses were also performed.

Results: The proinflammatory cytokines IL-6 and IL-18 were decreased in the MVC and MVC/RAPA groups, and TNF-α was decreased in all therapeutic groups. Galactosidase beta-1, a senescence biomarker, was also significantly reduced in all therapeutic groups, as were NK-kB1 and NF-kB2. In all groups, mTOR and CCL5 were significantly reduced. CCR5 expression was decreased in the MVC and MVC/RAPA groups.

Conclusions: MVC and RAPA may protect against some factors involved in liver aging. More studies will be necessary to verify their clinical applications.

Introduction

Aging leads to the progressive impairment of homeostasis at the cellular, tissue and organism levels, which reduces survival while increasing the risk of disease and death (1). In this context, aging is more influential than any other risk factor for the development of chronic diseases such as neurodegenerative diseases, cardiovascular diseases, diabetes mellitus, osteoporosis or cancer. There is considerable overlap between the hallmarks of aging and the pathogenic mechanisms of these diseases (1).

The immunological changes associated with aging are characterized by a chronic low-grade inflammatory state (inflammaging) (2). This inflammatory phenotype is associated with increases in inflammatory biomarkers such as C-reactive protein (CRP), interleukin-6 (IL-6), or tumor necrosis factor-alpha (TNF-α), which are associated with increased morbidity and mortality in older patients (2).

The liver is a key metabolic organ that governs energy metabolism. The liver acts as a hub to metabolically connect various tissues, including skeletal muscle and adipose tissue (3). On the other hand, the dysregulation of liver metabolism contributes to common aging-related diseases, such as insulin resistance, diabetes mellitus, and nonalcoholic fatty liver (4-5).

The aging process in the liver is driven by alterations in the genome that contribute to the dysregulation of mitochondrial function and nutrient sensing pathways, leading to cellular senescence and low-grade

inflammation (6). Moreover, the deterioration of metabolic pathways in the aging liver may be related to the senescence of hepatocytes. Senescent hepatocytes have altered expression of insulin metabolic pathways (7), as well as other genes involved in hepatic metabolism of glucose, lipids and proteins (7). Another principal characteristic of senescent cells is the increased activity of lysosomal β-galactosidase, which is also known as senescence-associated β-galactosidase (SA-β-gal). In diverse types of senescent cells, SA-β-gal is a widely used marker for identifying senescence *in vitro* and *in vivo* and is linked to the increased levels of lysosomes (8). In this context, senescent hepatocytes release proinflammatory cytokines such as IL-6, TNF-α, and IL-8 that are related to age-related inflammation (9).

IL-10 homozygous knockout (IL-$10^{tm/tm}$ [IL10KO]) mice are an excellent tool for the study of aging (10). In this mouse model, the inflammatory signaling pathway, specifically IL-10, has been interfered with (11). This cytokine has anti-inflammatory activities because it suppresses the activation of macrophages and inhibits the production of inflammatory cytokines by Th1 cells (12), giving rise to a mouse model with an accelerated aging phenotype (13).

Increasing evidence suggests that aging is a regulated process, and its course can be modified by modulating signal transduction pathways (14). Maraviroc (MVC), a specific CCR5 antagonist that is currently approved for clinical use, has exhibited some beneficial effects on certain factors involved in the development of frailty in mice (20). Rapamycin (RAPA), a macrolide antibiotic with antiproliferative properties, is a specific inhibitor of the mammalian target of rapamycin (mTOR) pathway (15). RAPA not only extends the lifespan of mice but also affects a variety of aging-related conditions in old mice (16). Indeed, RAPA can decrease C-C chemokine receptor type 5 (CCR5) mRNA expression (17), which is overexpressed in patients with frailty (18). Studies by our group examined murine models of liver damage and observed that animals treated with MVC exhibited a better anti-inflammatory profile than control animals (4, 19). Therefore, in the present study, our objective was to evaluate the effects of MVC and/or RAPA on liver tissue in an experimental model of aging in mice.

Materials And Methods

The Materials and Methods section has been published elsewhere (20). Briefly, a total of 80 male homozygous IL-10-deficient mice (B6.129P2-IL10tm1Cgn/J) were purchased from Jackson Laboratory (Bar Harbor, ME, USA). When the animals were approximately 6 weeks old, they were randomly assigned (n = 20) to one of 4 groups and fed for 24 weeks: i) the IL-10KO group (IL-10KO) received a standard rodent diet and tap water; ii) the preventive MVC group received the same diet as the IL-10KO group and were administered MVC (Pfizer, New York, N York) in their drinking water (300 mg/L) (4, 19, 20); iii) the preventive RAPA group received the same diet as the IL-10KO group and were administered RAPA in their drinking water (1.5 mg/kg/day) (20); and iv) the preventive MVC plus RAPA group (MVC-RAPA) received the same diet as the IL-10KO group and were administered MVC plus RAPA in their drinking water at the same concentration as in the MVC and RAPA groups.

The mice were observed daily, and all observations were recorded. All animals were sacrificed at Week 24. Blood samples were collected under anesthesia after a 4-hour fasting period. Internal organs were examined macroscopically and weighed.

Gene expression quantification

Total RNA was extracted and purified from liver samples using an RNA RNeasy Mini Kit (Qiagen, Valencia, CA) and treated with DNase I (Qiagen) according to the manufacturer's instructions. cDNA was synthesized by reverse transcription

of 1 mg of total RNA using the SuperScript III First-Strand Synthesis kit (Invitrogen, Carlsbad) in a total volume of 20 µl according to the manufacturer's instructions, followed by amplification using SYBR Green (Takara Bio Inc, Shiga, Japan) The PCR primer sequences are listed in Supplemental Table 1. The amplification and detection of specific products were performed using an ABI PRISM 7300 system (Applied Biosystems, Foster City, CA, USA). All reactions were run in duplicate for each sample. The expression of respective genes was normalized to glyceraldehyde 3-phosphate dehydrogenase (GAPDH) as an internal control.

Western blot analysis

Liver samples were lysed using a homogenizer in RIPA lysis buffer (Sigma Aldrich, St. Louis, MO). The cell lysate was centrifuged at 10,000 g for 10 minutes at 4 °C. The concentration of total protein in each sample was determined by the Bradford method. 5´adenosine monophosphate-activated protein kinase (AMPK), phosphorylated AMPK (pAMPK), protein kinase-B (Akt), phosphorylated Akt (pAkt), nuclear factor-kB (NFKB), phosphorylated NFKB (pNFKB), mammaliam target of rapamycin (mTOR) and phosphorylated mTOR (pmTOR) were evaluated by Western blotting (WB). GAPDH was used as an internal control (Supplemental Table 2).

Proteins were analyzed by colorimetry using a secondary antibody bound to peroxidase (anti-rabbit IgG, Cell Signaling, Danvers, MA) and incubated with the corresponding substrate. After high-resolution scanning, the concentration of each protein was evaluated by densitometry using Image J software. The density values for each of the test samples were normalized to the values of GAPDH, which was used as a loading control.

Histopathological Studies

Hematoxylin-eosin (HE) Staining

Following fixation, tissues were dehydrated and embedded in paraffin. Tissue sections (3 mm thick) were rehydrated and stained with HE according to standard protocols.

Immunohistochemical Analysis of Ki67

Deparaffinized sections were hydrated in a graded series of alcohol solutions. The sections were incubated in antigen retrieval buffer (the sections were boiled at 98 °C for 20 minutes in 10 mmol/L sodium citrate buffer) and treated with 3% H_2O_2 to block endogenous peroxidase. A monoclonal antibody (anti-Ki67, Santa Cruz Biotechnology, Inc.) was applied to the slides and incubated in a humidified chamber overnight in a refrigerator at 4 °C. Biotinylated secondary antibodies were then applied, followed by incubation with streptavidin peroxidase. The sections were washed with phosphate-buffered saline (PBS) three times after each step. The sections were stained with diaminobenzidine (DAB) chromogen solution and counterstained with hematoxylin.

Statistical analysis

The data are presented in the figures as the mean ± SEM (standard error of the mean). Body weight data were analyzed with analysis of variance followed by the Dunnett post hoc test. For all other data, the Kruskal–Wallis test was used followed by the Mann–Whitney U test. Correlations between variables were determined using the Spearman rank-sum test. All data were analyzed with GraphPad Prism 6 software and were considered statistically significant when $p<0.05$.

Results

Effects on proinflammatory cytokines

Compared to that in the control group, the IL-6 level was significantly lower in the MVC and MVC/RAPA groups ($p<0.05$ in both). The RAPA group also showed a clear tendency toward lower levels ($p=0.07$) (Figure 1). The expression of TNF-α was significantly lower in the MVC ($p<0.0001$), RAPA ($p<0.05$) and MVC/RAPA groups ($p<0.01$). In addition, the levels of IL-18, another proinflammatory cytokine, were also significantly lower in the MVC ($p<0.01$) and MVC/RAPA groups ($p<0.05$). IL-1β, another proinflammatory cytokine was examined, and the MVC group showed a tendency toward lower levels ($p=0.07$) (Figure 1).

Effects on chemokines

Compared to that in the control group, Chemokine (C-C) ligand 5 (CCL5) expression was lower in the MVC ($p<0.0001$), RAPA ($p<0.02$) and MVC/RAPA groups ($p<0.02$) (Figure 1). On the other hand, liver CCR5 expression was significantly reduced in the MVC (<0.0005) and MVC/RAPA groups ($p<0.0001$) (Figure 1).

Other biomarkers

Levels of mTOR were notably reduced in the RAPA and MVC/RAPA groups ($p<0.01$ and $p<0.05$, respectively), and there was a clear trend in the MVC group ($p=0.07$) (Figure 2). Galactosidase beta-1 (GLB-1) was also significantly reduced in the MVC ($p<0.01$), RAPA ($p<0.001$) and MVC/RAPA groups ($p<0.001$). NF-kB1 was examined, and the levels were significantly reduced in the MVC ($p<0.05$), RAPA ($p<0.01$) and MVC/RAPA groups ($p<0.05$). A similar outcome was observed regarding liver expression of NF-kB2 in the MVC ($p<0.01$), RAPA ($p<0.05$) and MVC/RAPA groups ($p<0.05$) (Figure 2).

Western blot analysis

Mice treated with MVC showed significant increases in total NF-kB ($p < 0.05$), p-Akt ($p < 0.05$) and p-mTOR ($p<0.01$). In addition, the RAPA group showed an increase in p-NFKB ($p<0.01$). The MVC-RAPA group showed a significant increase in p-Akt ($p < 0.05$), p-mTOR ($p < 0.001$) and p-AMPK ($p<0.01$) (Figure 3).

Histopathological assessment of liver tissue

No differences were observed after analyzing HE staining and immunohistochemical analysis of Ki67 (data not shown).

Discussion

Most chronic human diseases increase with age (20). This makes it important to look for different strategies to reduce aging. However, murine models cause pathology in young mice. It is known that the lifespan of mice can be modified by dietary, genetic, and pharmacological interventions (21). Exciting findings have shown that rodent aging can be accelerated, stopped, or reversed simply by altering the systemic environment (22). This growing line of research may offer strategies for treating aging. In this context, RAPA was the first drug to dramatically slow aging in mice (23). RAPA also increases life expectancy in most studies and protects against many age-related diseases (23). Other drugs, such as metformin and acarbose, also prolong the lifespan of mice (24, 25). MVC also has some potential benefits on aging because it modifies certain factors involved in the development of frailty in mice, such as myostatin and certain inflammatory cytokines (20). mTOR has been implicated in many of the processes associated with aging, including cell senescence, immune responses, cell stem regulation and mitochondrial function (26). Inhibiting mTOR with RAPA delays aging and increases lifespan (15). In our study, MVC, RAPA or MVC-RAPA reduced the levels of mTOR. Consistent with this observation, there is evidence of decreased mTOR activity, at least in the liver, in mice in which the aging process has been delayed, such as due to gene mutations (16). In our study, all mice that were treated with MVC-RAPA showed higher protein levels of p-mTOR. The phosphorylation of mTOR by Akt occurs directly via Rheb (Ras family of GTPase) (27). There are transcription factors that can be activated or inhibited after the phosphorylation of the Akt pathway (27). In our study, both MVC and MVC/RAPA activated this metabolic pathway. In addition to activated Akt, inflammatory and oxidative stress stimulate the NF-kB family of transcription factors (28). In mouse models, the inhibition of NF-kB has been shown to lead to late onset of age-related symptoms because most of the genes under the transcriptional control of NF-kB are involved in biologic pathways associated with aging, including immune responses, cell senescence, apoptosis and metabolism (29). All of these factors contribute to age-related tissue degeneration (2). These changes have been described in liver tissue from mice and rats (6). Our results showed that at the mRNA level, there was a decrease in NF-kB expression in the liver (1&2) in all therapeutic groups, while at the protein level, there was an increase in total NF-kB expression in the MVC group. This increase was the same as that observed in the muscles of aged IL-10 mice (20). NF-kB activation is related to many of the known lifespan regulators, including mTOR (28). Therefore, NF-kB represents a potential antiaging

therapeutic target. Consistent with our results, mTOR and NF-kB signaling are coregulated (30). Another component that contributes to the increase in NF-kB activity that is associated with aging is control of the expression of inflammatory cytokines (31). Increasingly, inflammation is being linked to aging and chronic diseases (32). The basal inflammatory response increases with age, leading to low-level chronic inflammation that is likely maladaptive and promotes aging. In this animal model of aging, we observed changes in the levels of proinflammatory cytokines (IL-6, TNF-α, and IL-18). Therefore, the main protective effect of MVC and RAPA depends on a proinflammatory pathway. This inflammatory phenotype accelerates aging.

Another biomarker of aging is the activity of β-gal in senescent cells, which is related to lysosomal activity (8). Cellular senescence impairs tissue regeneration and drives chronic low-grade inflammation, which exacerbates the aging process (33). In our study, all the therapeutic groups showed reduced GLB-1 expression in the liver, reducing senescence and low-grade chronic inflammation.

To better understand the mechanism underlying these observations, in this animal model, we did not observe a synergistic, additive or antagonistic effect on the levels of CCR5 or CCL5 mRNA in the liver in the MVC-RAPA group. CCL5 plays an active role in the recruitment of a variety of leukocytes to inflammatory sites, including T cells, macrophages, eosinophils, and basophils (17). In collaboration with certain cytokines that are released by T cells, such as IL-2 and Interferon gamma (IFN-γ), CCL5 induces the activation and proliferation of certain natural killer cells to generate chemokine-activated C-C killer cells (34). CCL5/CCR5 interactions can act as growth factors, inducing the recruitment of additional inflammatory cells and participating in immune evasion (18).

In summary, our data suggest that the use of MVC and/or RAPA could have protective effects on some factors involved in liver aging. Additional studies will be necessary before justifying a randomized, controlled trial to determine their beneficial effects.

Abbreviations

MVC: Maraviroc

RAPA: Rapamycin

CRP: C-reactive protein

IL-6: Interleukin-6

TNF-α: Tumor necrosis factor-alpha

SA-β-gal: Senescence-associated β-galactosidase

mTOR: Mammaliam target of rapamycin

CCR5: C-C chemokine receptor type 5

GAPDH: Glyceraldehyde 3-phosphate dehydrogenase

AMPK: 5´adenosine monophosphate-activated protein kinase

Akt: Protein kinase-B

NF-kB: Nuclear factor-kB

WB: Western blotting

HE: Hematoxylin-eosin

PBS: Phosphate-buffered saline

DAB: Diaminobenzidine

SEM: Standard error of the mean

CCL5: Chemokine (C-C) ligand 5

GLB-1: Galactosidase beta-1

Declarations

Ethics approval and consent to participate:

All procedures were carried out in accordance with the European Communities Council Directive (86/609/CEE) on animal experiments and with approval from the ethical committee on animal welfare of our institution (Comité Etico de Experimentación Animal del Centro de Investigación Biomédica de La Rioja, CEEA-CIBIR). Consent to participate not applicable.

Consent to publication: Not applicable.

Availability of data and materials: The authors of this manuscript understand that materials and results described in this manuscript, including all relevant raw data, will be freely available to any scientist.

Competing interests: All authors have read the journal's authorship agreement and policy on disclosure of potential conflicts of interest. Dra. L. Pérez-Martínez has received compensation for lectures from Abbvie, Bristol-Myers Squibb, Gilead Sciences, and Janssen. Dr. J. R. Blanco has carried out consulting work for Abbvie, Bristol-Myers Squibb, Gilead Sciences, Janssen, Merck, ViiV Healthcare and THERA technologies; has received compensation for lectures from Abbvie, Bristol-Myers Squibb, Gilead Sciences, Janssen, Merck, and ViiV Healthcare, as well as grants and payments for the development of educational presentations for Gilead Sciences, Bristol-Myers Squibb and ViiV Healthcare. The rest of the authors declare no conflict of interest.

Funding: This study was partially supported by the Instituto de Salud Carlos III (ISCIII), M. Economía y Competitividad of Spain [Project Fondo de Investigaciones Sanitarias PI16/00127 (Acción Estratégica en Salud 2013-2016)]. Co-funded by European Regional Development Fund (FEDER) "A way to make Europe", by the Fondos FEDER, Convocatoria de ayudas a grupos de investigación para el desarrollo de proyectos de investigación, desarrollo tecnológico e innovación en el sector biomédico (Convocatoria FEDER-La Rioja; FRSABC007), and RTI2018-097455-B-I00 (MCIU/AEI/FEDER, UE); CIBER de Cáncer (CB16/12/00275).

Author contributions: Conceived and designed the project: LPM, JRB, AC, LR, EMVS, SMG. Performed the experiments: LPM, LR, EMVS, SM, AA. Analyzed the data: LPM, JRB, AC, LR, EMVS, SMG, SRM, AA. Wrote the paper: LPM.

Acknowlegments:

Maraviroc and Rapamycin, were a generous gift from Pfizer.

References

1. Niccoli T, Partridge L. Ageing as a risk factor for disease. Curr Biol. 2012; 22; 41-52.
2. Franceschi C, Bonafè M, Valensin S, Olivieri F, De Luca M, Ottaviani E, et al. Inflamm-aging. An evolutionary perspective on immunosenescence. Ann N Y Acad Sci. 2000; 908:244-254.
3. Trefts E, Gannon M, Wasserman DH. The liver. Curr Biol. 2017; 6: 1147–51.
4. Perez-Martinez L, Perez-Matute P, Aguilera-Lizarraga J, Rubio-Mediavilla S, Narro J, et al. Maraviroc, a CCR5 antagonist, ameliorates the development of hepatic steatosis in a mouse model of non-alcoholic fatty liver disease (NAFLD). J Antimicrob Chemother. 2014; 69:1903–10.
5. Papatheodoridi AM, Chrysavgis L, Koutsilieris M, Chatzigeorgiou A. The Role of Senescence in the Development of Nonalcoholic Fatty Liver Disease and Progression to Nonalcoholic Steatohepatitis. Hepatology. 2020; 71:363-374.
6. Hunt NJ, Kang SWS, Lockwood GP, Le Couteur DG, Cogger VC. Hallmarks of Aging in the Liver. Comput Struct Biotechnol. J 2019: 7; 1151-61.
7. Aravinthan A, Challis B, Shannon N, Hoare M, Heaney J, Alexander JMG. Selective insulin resistant in hepatocyte senescence. Exp Cell Res. 2015; 331: 38-45.
8. Debacq-Chainiaux F, JD Erusalimsky, J Campisi, Toussanit O. Protocols to detect senescence-associated beta-galactosidase activity (SA-betagal), a biomarker of senescent cells in culture and in vivo. Nat Protocol. 2009; 4: 1798–1806.
9. Lasry A, Ben-Neriah Y. Inflammatory responses associated with senescence: perspectives on aging and cancer. Trends Immunol. 2015; 36: 217-228
10. Kõks S, Dogan S, Tuna BG, González-Navarro H, Potter P, Vandenbroucke RE. Mouse models of ageing and their relevance to disease. Mech Ageing Dev. 2016; 160:41-53.

11. Walston J, Fedarko N, Yang H, LLeng S, Beamer B, Espinoza S, et al. The physical and biological characterization of a frail mouse model. J Gerontol A Biol Sci Med Sci. 2008; 63:391–398.
12. Fiorentino, DF, Zlotnik, A, Mosmann, TR, Howard M, O´Garra A. IL-10 inhibits cytokineproduction by activated macrophages. J. Immunol. 1991: 147: 3815–22.
13. Kühn R, Löhler J, Rennick D, et al. Interleukin-10-deficient mice develop chronicenterocolitis.Cell.1993;75:263-274.
14. Mannic JB, Morris M, Hockey HP, Roma G, Beibel M, Kulmatycki K, et al. TORC1 inhibition enhances immune function and reduces infections in the elderly.SciTransMed.2018;10:eaaq1564.
15. Harrison DE, Strong R, Sharp ZD, Nelson JF, Astle CM, Flurkey K, et al. Rapamycin fed late in life extends lifespan in genetically heterogeneous mice. Nature. 2009; 460:392–395.
16. Wilkinson JE, Burmeister L, Brooks SV, Chan CC, Freidline S, Harrison DE et al. Rapamycin slows aging in mice. Aging Cell. 2012; 11:675–682.
17. Gilliam BL, Riedel DJ, Redfield RR. Clinical use of CCR5 inhibitors in HIV and beyond. J Transl Med. 2011; 9 Suppl 1:S9.
18. De Fanis U, C. Wang G, NS. Fedarko, Walston JD, Casolaro V, Leng SX. T-lymphocytes expressing CC chemokine receptor-5 are increased in frail older adults. J Am Geriatr. 2008; 56:904-908.
19. Ochoa-Callejero L, Pérez-Martínez L, Rubio-Mediavilla S, Oteo JA, Martínez A, Blanco JR. Maraviroc, a CCR5 antagonist, prevents the development of hepatocellular carcinoma in a model of mouse. PLoS One. 2013; 8: e53992.
20. Pérez-Martínez L, Romero L, Muñoz-Galván S, Verdugo-Sivianes EM, Rubio-Mediavilla S, Oteo JA, et al. Implications of maraviroc and/or rapamycin in a mouse model of fragility. Aging (Albany NY). 2020:12;8565-82.
21. Kennedy BK, Pennypacker JK. Drugs That Modulate Aging: The Promising yet Difficult Path Ahead. Transl Res. 2014; 163: 456–465.
22. Rando TA, Wyss-Coray. Stem cells as vehicles for youthful regeneration of aged tissues. Gerontol A Biol Sci Med Sci. 2014; 69 Suppl 1:39–42.
23. Johnson SC, Rabinovitch PS and Kaeberlein M. mTOR is a key modulator of ageing and age-related disease. Nature. 2013: 17; 493: 338–345.
24. Harrison DE, Strong R, Allison DB, Ames BN, Astle CM, Atamna H et al. Acarbose, 17-α-estradiol, and nordihydroguaiaretic acid extend mouse lifespan preferentially in males. Aging Cell. 2014; 13: 273–282.
25. Martin-Montalvo A, Mercken EM, Mitchell SJ, Palacios HH, Mote Pl, Scheibye-Knudsen M et al. Metformin improves healthspan and lifespan in mice. Nat Commun. 2013; 4: 2192.
26. Papadopoli D, Boulay K, Kazak L, Pollak M, Mallette F, Topisirovic I, et al. mTOR as a central regulator of lifespan and aging. F1000Res 2019: 8: F1000 Faculty Rev-998.
27. Yang H, Jiang X, Li B, et al. Mechanisms of mTORC1 activation by RHEB and inhibition by PRAS40. Nature. 2017: 552: 368-373.

28. Salminen A and Kaarniranta K. NF-kappaB signaling in the aging process. J Clin Immunol. 2009, 29:397-405. https:// doi: 10.1007/s10875-009-9296-6. 29- Adler A, Sinha S, Kawahara LA, Zhang JY, Segal E, Chang HY. Motif module map reveals enforcement of aging by continual NF-kappaB activity. Genes Dev. 2007: 21:3244-57.
29. Dan HC and Baldwin AS. Differential involvement of IkappaB kinases alpha and beta in cytokine- and insulin-induced mammalian target of rapamycin activation determined by Akt. J Immunol. 2008, 180:7582-89.
30. Coppe JP, Patil CK, Rodier F, Krtolica A, Beauséjour CM, Parrinello S, et al. A human-like senescence-associated secretory phenotype is conserved in mouse cells dependent on physiological oxygen. PLoS One. 2010;5:e9188.
31. Salvioli S, Monti D, Lanzarini C, Conte M, Pirazzini C, Bacalini MG, et al. Immune system, cell senescence, aging and longevity–inflamm-aging reappraised. Curr Pharm Des. 2013;19:1675-79.
32. Childs BG, Gluscevic M, Baker DJ, Laberge RM, Marquess D, Danaberg J, et al. Senescent cells: an emerging target for diseases of ageing. Nat Rev Drug Discov. 2017:16: 718–735.
33. Soria G and Ben-Baruch A. The inflammatory chemokines CCL2 and CCL5 in breast cancer. *Cancer Letters.* 2008; 267:271–285.

Figures

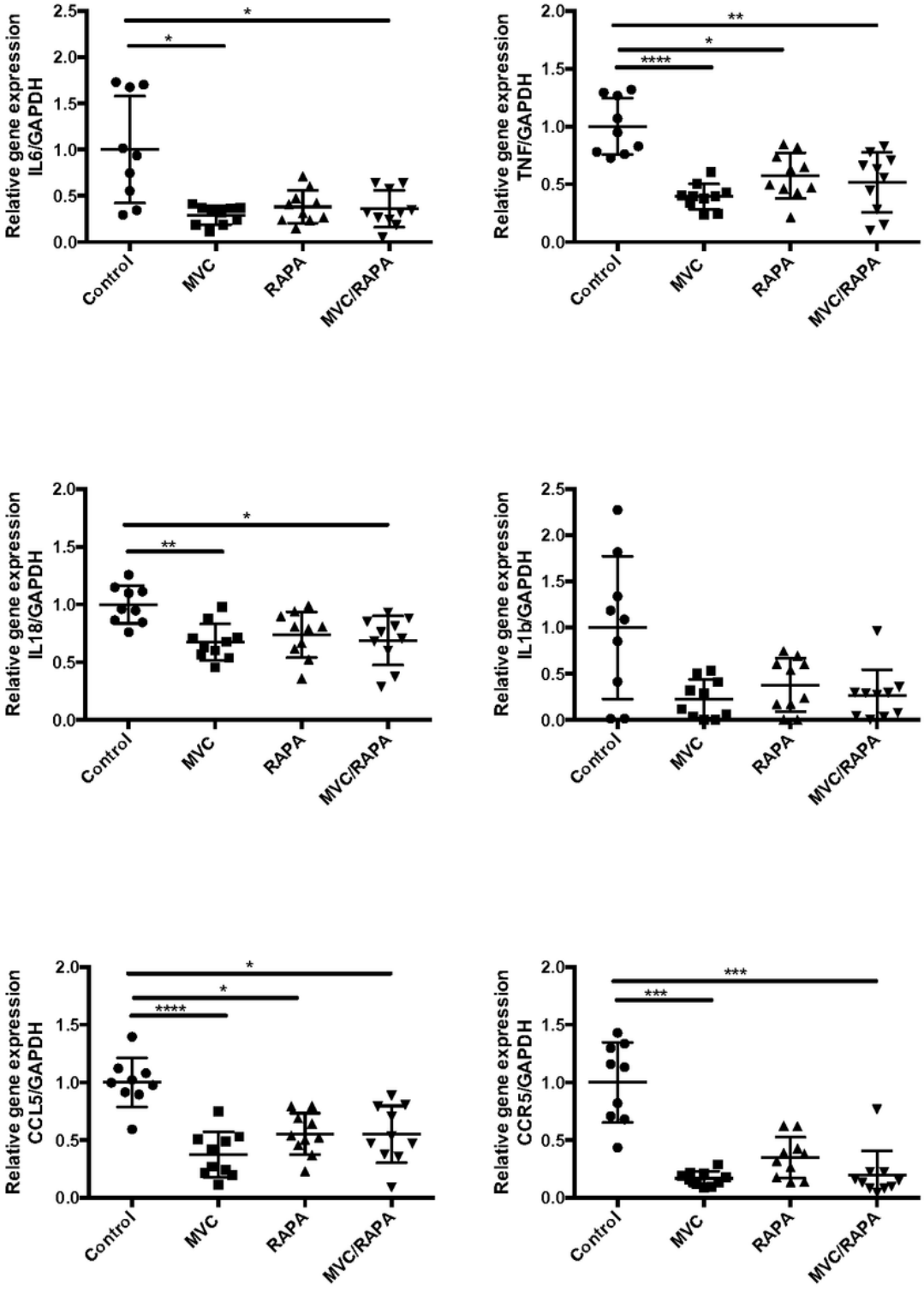

Figure 1

Liver expression of IL-6, TNF-α, IL-18, IL-1β, CCL5 and CCR5 at the RNA level.

(**A**) Although IL-6 expression was lower in all the therapeutic groups; it was only statistically in MVC and MVC/RAPA group. (**B**) There was a significant decrease of TNF-α expression in all therapeutic groups. (**C**) IL-18 was significantly reduced in MVC and MVC/RAPA groups. (**D**) No differences were observed after

analyzing IL-1β, but all therapeutic groups were lower than the control group. (**E**) CCL5 expression was significantly lower in all the therapeutics groups. (**F**) CCR5 expression was statistically significant lower in MVC and MVC/RAPA groups Each bar represents the mean ± SEM. *p<0.05, **p<0.01. ***p<0.001 and ****p <0.0001 with respect to control. MVC, maraviroc. RAPA, rapamycin. MVC/RAPA, maraviroc plus rapamycin. IL, interleukin. TNF-α, tumor necrosis factor-alpha.

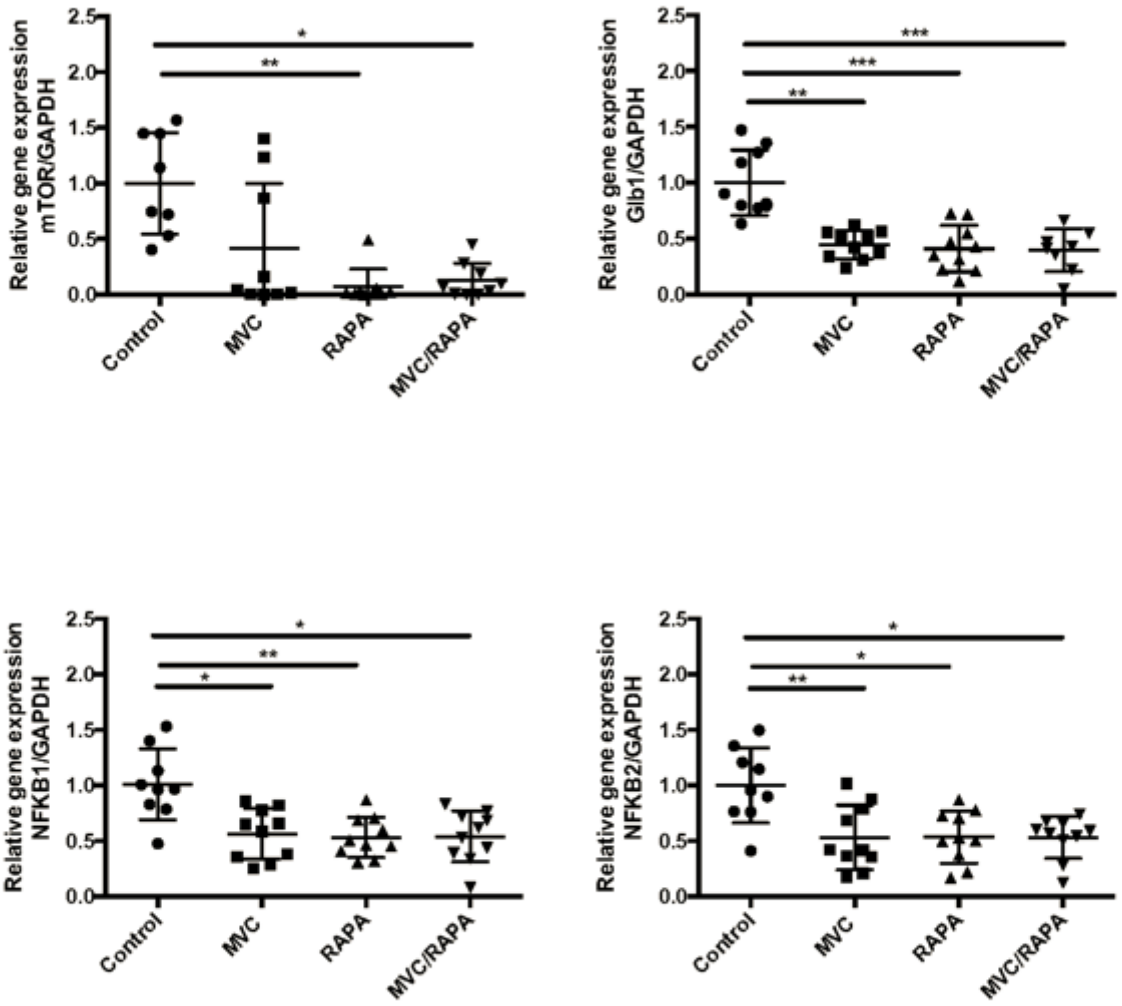

Figure 2

Liver expression of mTOR, GLB-1 and nuclear factor KB 1and 2 at the RNA level.

(**A**) A significant decrease of mTOR expression was recorded in all groups, but it was statistically significant in RAPA and MVC/RAPA groups. (**B**) There was a significative decrease of GLB-1 in all the therapeutic groups. (**C**) NF-kB1 and (**D**) NF-kB2 were statistically significant in all therapeutic groups. Each bar represents the mean ± SEM. *p<0.05, **p<0.01 and ***p<0.001 with respect to control. MVC, maraviroc. RAPA, rapamycin. MVC/RAPA, maraviroc plus rapamycin. mTOR, mammalian Target of Rapamycin. GLB-1, Galactosidase Beta-1. NF-kB, nuclear factor KB.

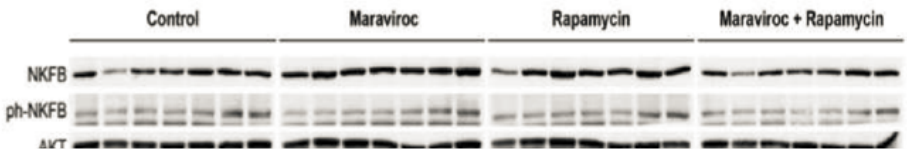

Figure 3

Analyses of the molecular pathways involved in the mechanism of action of MVC and RAPA.

(**A**) Western blot analysis of the protein levels of NF-KB (total and phosphorylated), AKT (total and phosphorylated), mTOR (total and phosphorylated), AMPK (total and phosphorylated), GAPDH as endogenous control, in mice treated with maraviroc (MVC group), Rapamycin (RAPA group) or combination of both (MVC-RAPA group). (**B**) Box plots showing the average protein levels. Data were analyzed using Student t test´s. *, P<0.05; **, P<0.01; ***, P<0.001.

Supplementary Files

This is a list of supplementary files associated with this preprint. Click to download.

- SupplementalTable1.docx
- SupplementalTable2.docx